

# On the outburst light curves of soft X-Ray transients as response of the accretion disk to mass deposition

Ünal Ertan and M. Ali Alpar

Physics Department, Middle East Technical University, Ankara 06531, Turkey  
ertan@newton.physics.metu.edu.tr  
alpar@newton.physics.metu.edu.tr

May 29, 2017

**Abstract.** We note that the solution of accretion disk dynamics for an initial delta-function mass distribution gives a light curve that fits both the rise and the decay pattern of the outburst light curves of black-hole soft X-ray transients (BSXTs) until the onset of the first mini outburst quite well. The Green's function solution of Lynden-Bell & Pringle (1974) is employed for two different time-independent viscosity laws to calculate the expected count rates of X-ray photons in the Ginga energy bands as a function of time. For both models basic characteristics of the outburst light curves of two typical sources GS 2000+25 and GS/GRS 1124-68 are reproduced together with plausible values of the thin disk parameter  $\alpha$  and the recurrence times. This agreement with the outburst light curves and the source properties during quiescence support the idea of mass accumulation and the sporadic release of accumulated mass at the outer disk.

**Key words:** Soft X-ray transients, accretion discs - black-holes, X-rays

monotonic decline in many cases there is more complex behavior. Some sources remain persistent for more than one year. Most of the light curves show a steepening around  $10^{36}$  erg s<sup>-1</sup> corresponding to a mass accretion rate  $\dot{M}_x \sim 10^{16}$  g s<sup>-1</sup> inferred from the X-ray luminosity. Later they turn back to their quiescent states with  $L_x \sim 10^{31} - 10^{33}$  erg s<sup>-1</sup> and  $\dot{M}_x \sim 10^{11} - 10^{13}$  g s<sup>-1</sup> (Tanaka & Shibazaki 1996 and references therein).

There are nine known X-ray binaries with strong black-hole candidate primaries (van Paradijs 1995). Three of these sources are non-transient high mass systems and the remaining six are transient LMXBs (Table 1). Four BSXTs in this group, A0620-00, GS 2000+25, GS/GRS 1124-68 and GRO J0422+32 show striking similarities. Their outbursts have fast rise times around a few days. The decay phases can be fit with exponentials with time constants around one month. During decline all four sources exhibit secondary (mini) outbursts. A0620-00, GS/GRS 1124-68 show also tertiary outbursts. The tertiary outburst is absent in the light curve of GRO J0422+32, but it may also be present in GS 2000+25. Secondary maxima were detected around 80 days after the onset of the main outburst of GS 2000+25 and GS/GRS 1124-68. A0620-00 and GRO J0422+32 exhibited the secondary maxima 50 days and 125 days after the onset respectively. For both GS 0620-00 and GS/GRO 1124-68 the tertiary maxima were observed about 200 days after the onset of the main outburst (Tanaka & Shibazaki 1996). The basic features of the mini outbursts are the sharp increase in luminosity by a factor of  $\sim 1 - 3$  and decay patterns which mimic the decay after the first outburst. A0620-00 is a recurrent transient with a recurrence time of 58 years (Tsunemi et al 1989). The outbursts of the other sources were detected only once putting a lower limit to their recurrence times of around a few ten years (see Table 1). These similarities allow the working hypothesis that all of these sources run with a similar mechanism.

## 1. Introduction

About two thirds of the known LMXBs are persistent and the remaining one third are transient sources (van Paradijs 1995). The transient sources exhibit a soft X-ray spectrum during outbursts (soft X-ray transients -SXTs). An optical outburst also occurs together with the X-ray outburst. During an outburst the X-ray and the optical properties of black-hole soft X-ray transients (BSXTs) and neutron star soft X-ray transients (NSXTs) are very similar to each other and also to those of persistent sources. X-ray luminosities of SXTs increase from below  $10^{33}$  erg s<sup>-1</sup> to  $\sim 10^{37}$ - $10^{38}$  erg s<sup>-1</sup> during an outburst. The time scales for decline range from several tens of days to more than one hundred days. Although some sources show rather

Since the conditions for outburst build up in the quiescent state it is important to treat the observations made during quiescence. According to the standard disk model (Shakura & Sunyaev 1973) most of the X-rays ( $> 70\%$ ) come from the inner parts of the disk extending to a radius which is around ten times the radius of the last stable orbit,  $R_0 = 3R_g = 3(2GM_X/c^2)$ . During the quiescent state it is possible to fit a black-body curve roughly to the observed X-ray spectrum. However, inner disk temperatures of  $\sim 0.2 - 0.3$  keV obtained from these fits give very small values ( $1 - 10$  km<sup>2</sup>) for the X-ray emitting area of the disk, while realistic areas imply temperatures that are orders of magnitude smaller than the soft X-ray temperatures that fit the spectra. A disk becomes optically thin below a certain accretion rate depending on the viscosity parameter  $\alpha$  (Shakura & Sunyaev 1973). An optically thin or gray disk may be one way of explaining this inner disk problem.

The mass accretion rates obtained from the optical observations during quiescence ( $\sim 10^{15} - 10^{16}$  g s<sup>-1</sup>) are orders of magnitude larger than those ( $\sim 10^{11} - 10^{13}$  g s<sup>-1</sup>) obtained from the X-ray luminosities (see, e.g., McClintock et al 1995, for these questions in A0620-00).

An advection dominated inner disk has been proposed to account for the properties of BSXTs. According to this model most of the energy released in the inner disk is advected into the compact star instead of being radiated from the disk (Narayan et al 1996). Regarding the difference between mass accretion rates obtained from optical and X-ray luminosities during the quiescent states, the NSXTs are similar to BSXTs. Although this model could explain the observed spectra and also the low X-ray luminosities of BSXTs in quiescence it is not able to explain the properties of NSXTs because of the existence of the solid surfaces of the neutron stars: Whatever the disk structure is matter finally reaches the neutron star surface which should produce a distinct black-body like emission.

Another possibility is mass accumulation in the outer regions of the disk. This accumulated matter may be the source of the outburst. For both BSXTs and NSXTs, the mass accretion rate inferred from optical observations may indicate the mass accretion rate arriving to accumulate in the outer disk, while the much lower  $\dot{M}_X$  inferred from the X-ray luminosity may reflect the trickle of mass that proceeds through a mass-starved inner disk characteristic of the quiescent state. This qualitative picture would persist until the mass accumulated in the outer disk reaches the level critical for an outburst.

Models for SXTs must address the characteristic time scales: (1) Fast rise of the light curves around a few days; (2) The subsequent decay with a time scale of the order of one month; (3) Recurrence times of the order of a few ten years. Further, as viscosity is involved in determining the decay, values of the viscosity parameter must be plausible. For comparison  $\alpha \sim 0.1 - 1$  for dwarf novae and related

systems for the reaction time of the disk to be  $10^5 - 10^6$  s (Bath & Pringle 1981).

There are mainly two types of models for SXTs: the disk instability models (DIM) (e.g. Meyer & Meyer-Hofmeister 1981; Mineshige & Wheeler 1989; Cannizzo 1992; Cannizzo et al 1995 (CCL)) and the mass transfer instability models (MTI) (e.g. Hameury et al 1986; 1987; 1988; 1990).

The basic idea for MTI is that the accretion from the secondary star is unstable for a range of accretion rates roughly from  $\sim 10^{12} - 10^{15}$  g s<sup>-1</sup> to  $\sim 10^{16} - 10^{17}$  g s<sup>-1</sup>. The secondary star expands under the influence of hard X-rays ( $E > 7$  keV) from the primary. The accretion rate exceeds the upper limit of the lower stable range and jumps to an accretion rate greater than the minimum of the higher stable range. The subsequent burst of mass flow produces the outburst. The disk becomes thicker and thicker, finally shielding the region around the  $L_1$  point. When the X-ray illumination stops the companion shrinks and the system returns to its quiescent state. MTI models produce the basic characteristics of the light curves and the recurrence times. The problem with MTI is that, according to the model, the hard X-ray flux with  $E > 7$  keV must exceed  $\sim 2.5 \times 10^{34}$  ( $M_c/M_\odot$ )<sup>2</sup> erg s<sup>-1</sup> in the quiescent state (Hameury et al. 1986) while there is no data showing the existence of photons in this energy range with such high luminosities before the outbursts (Tanaka & Shibazaki 1996).

DIMs are highly accepted today, although they do not produce a completely self consistent picture explaining all features of SXTs. Initially DIMs were successful in explaining basic characteristics of dwarf novae (Cannizzo 1994). The model was extended to explain the behavior of SXTs which are similar to dwarf novae in some cases. The disk instability follows a limit cycle mechanism based on an "S" shaped surface density  $\Sigma$  versus  $\dot{M}$  curve. Upper and lower branches of the "S" correspond to hot and cool states respectively. The middle branch represents an unstable regime. When  $\dot{M} > \dot{M}_{min}$  the disk follows the upper branch switching to the lower branch when  $\dot{M} < \dot{M}_{max}$ . Each radius in the disk has its own "S" curve. If the mass transfer satisfies the condition  $\dot{M}_{max}(R_{inner}) < \dot{M}_T < \dot{M}_{min}(R_{outer})$  then the limit cycle mechanism operates through the range between  $R_{inner}$  and  $R_{outer}$ . If this range of radii covers the entire disk then the whole disk can jump from one stable branch to the other. Accumulation of matter at some radius  $R$  may cause mass per unit area  $\Sigma(R)$  to exceed  $\Sigma_{max}(R)$ . Viscous dissipation increases suddenly. Waves of surface density propagate to both smaller and larger radii. As a result, the surface density at each radius in the disk exceeds the maximum critical value of the lower branch, and the disk jumps to the hot branch. At the end of this process the disk finds itself in a high viscosity state. Unlike the quiescent state now the viscous time scale becomes small and matter flows on to the central object. Because of the

matter flow the densities in the outer regions decrease to below the critical densities. This causes a cooling front to propagate throughout the disk decreasing the local surface density at each radius to below the local critical values. Propagation of the cooling front means the decay of the outburst (e.g., Cannizzo 1992; Lasota et al 1996).

The main difficulty of this model is that the  $\alpha$  values needed in order to produce recurrence times of around a few ten years are not able to produce the observed amplitude and duration of the outbursts or vice versa (for a discussion of the problems see, e.g. Lasota 1996).

In this work BSXTs will be studied with a different approach concentrating on a simple explanation in terms of a disk dynamics model for both rise and the decay pattern of the light curves until the onset of the first mini outburst. We explore the behavior of the disk following a sudden release of mass in the outer radius in terms of the disk dynamics model of Lynden-Bell & Pringle (1974) (LP). The observations of GS 2000+25 and GS/GRS 1124-68 will be used to illustrate the model.

LP made a study for the evolution of viscous disks in general. In particular the solution with no central flux is of interest, corresponding to a disk with a black-hole at its center. The Green's function solution of LP take initial density distributions in the form of delta functions in radius. This is an idealization of an initial mass enhancement in a ring. Convolution of the elementary solution of this Green's function model with any initial mass distribution will give the general solution. Initial mass release at a thin ring at the outer radius (or at a specific radius in the disk) already corresponds to a solution with a single delta function initial mass distribution. Thus the Green's function solution of LP is taken here as the physical solution for the BSXT outbursts. The motivation leading us to this approach is the similarity between the observed X-ray light curves of the outbursts and the Green's function luminosity calculated by LP. This hypothesis means that a sudden dumping of mass in the outer disk leads to the observed outburst. The present work applies the model to the data from GS 2000+25 and GS/GRS 1124-68.

The part of the study by LP related to our application is summarized in the Appendix. In Section 2 data from GS 2000+25 and GS/GRS 1124-68 are examined with the model. The aim is to calculate the photon flux from the disk in the observed X-ray band of Ginga (1 – 20 keV) as a function of time using the LP model, and compare this with observed photon flux data taken with the Ginga satellite ( provided by S.Kitamoto, private communication). A good fit to the data until the first mini outburst is obtained (Figs. 1–4). From this fit the characteristics of the outburst, the viscosity parameter  $\alpha$ , the total mass released and the recurrence times will be obtained for both sources. Section 3 summarizes the conclusions, discusses the scope of the model and the problems, and tests for future applications, including the secondary and tertiary

maxima commonly seen in the decay phases of the outbursts of BSXTs.

## 2. Models For the X-Ray Light Curves of Black-hole Soft X-Ray Transients

LP present a luminosity versus dimensionless time,  $t_*$ , curve for the delta function initial condition. This curve is similar to the observed light curves of BSXTs. The similarity is attractive because a mass accumulation at the outer disk may also be represented by a delta function initial mass distribution. If a disk instability causes a transition to a high viscosity state so that the viscous time scale becomes short compared to that in the preoutburst state then a sudden release of mass would occur. For such a situation the Green's function solution with a delta function initial mass distribution would approximately describe the subsequent evolution of the disk.

To test this idea we consider a delta function initial mass distribution located at a radius  $R_1$ ,  $\Sigma(R_1, R, 0) = \delta m (2\pi R)^{-1} \delta(R - R_1)$ , and use the Green's function in Eq.(A.18) as the solution of our problem.  $\delta m$  is the mass which is initially injected at the outer radius  $R_1$ . The solution is equivalent to Eq.(A.18) except for a factor  $\delta m$  in front.

We try two viscosity models and compare the results to the observations. In the first model we choose the kinematic viscosity  $\nu$  to be constant for simplicity. In the second model we use the form of the viscosity parameter  $\alpha = \alpha_0(z_0/R)^n$  where  $z_0$  is the half thickness of the disk. This form is commonly used for the disk instability models. CCL succeeded to produce exponential decays of the light curves of BSXTs using this form with  $n = 1.5$ . For the LP model Eq.(A.10) is valid if  $\nu$  is time independent, and either independent of  $R$  or a power law function of  $R$ . On the other hand the general prescription of the kinematic viscosity is  $\nu = (2/3)(P/\rho)(\alpha/\Omega)$ . Since  $(P/\rho) \propto T$ ,  $\nu$  becomes independent of  $T(R, t)$  only when  $\alpha \propto T^{-1}$ . This choice corresponds to  $n = -2$  and leads  $\nu$  to be a function of the specific angular momentum  $h$  as we will discuss in the second model. For both models the photon flux is calculated as a function of time, as the injected mass at  $R_1$  spreads through the disk. The choice of  $\alpha \propto T^{-1}$  may not be physical. It is implemented here in order to apply the LP model. The success of the model may indicate that a real disk is effectively represented by the LP model with the artificial choices made here. Although a temperature and time independent viscosity is unrealistic, the success of the simple analytical LP solution in fitting the light curve motivates us to take this prescription as a useful effective representation. We shall discuss the viscosity parameter  $\alpha$ , the accumulated mass  $\delta m$  and the recurrence times using the two viscosity models.

The models discussed below are summarized in Tables (2–4)

**Table 1.** BSXTs with  $M_X > 3M_\odot$  (Ref: Tanaka & Shibazaki 1996 and references therein)

Name	BH mass ( $M_\odot$ )	Outburst year	$L_{ave}$ ( $10^{35}$ erg/s)	$\langle \dot{M} \rangle$ ( $10^{15}$ g/s)
J0422+32	> 3.2	1992	0.8	0.2
0620-00	> 7.3	1917,1975	2	2
1124-68	$\sim 6$	1991	7	7
J1655-40	4-5	1994	?	?
2000+25	6-13.9	1988	3	3
2023+33	8-15.5	1956,1979 ?	2 ?	2 ?
		1989	0.6	0.6

**MODEL I : Constant  $\nu$** 

We first investigate a model with  $\nu$  constant in time and uniform throughout the disk. We shall obtain limits on  $\nu$  by requiring that the (variable)  $\alpha$  parameter is less than one. If the initial mass distribution is given by Eq.(A.16) multiplied by  $\delta m$  the general time dependent solution for the couple is Eq.(A.18) multiplied by  $\delta m$  (see Appendix)

$$g = \delta m 2l\kappa^{-2} \frac{(x_1 x)^l}{x_1^2 t_*} \exp - \left[ \frac{(x_1 - x)^2}{2t_* x_1^2} \right] F_l \left( \frac{x/x_1}{t_*} \right) \quad (1)$$

where  $l$  is constant,  $x = h^{1/2l} = (\Omega R^2)^{1/2l} = (GM R)^{1/4l}$ ,  $t_* = 2\kappa^{-2} t / x_1^2$ ,  $F_l(z) = e^{-z} I_l(z)$ ,  $I_l(z)$  is the Bessel function of imaginary argument, and

$$\kappa^{-2} = 3 (GM)^2 \nu \quad (2)$$

The dimensionless time is

$$t_* = \frac{6\nu t}{R_1^2} \quad (3)$$

Substituting

$$\frac{dh}{d\Omega} = \frac{1}{2} (GM)^{1/2} R^{-1/2} \quad (4)$$

in Eq.(A.10) we have

$$\frac{3}{4} (GM)^2 \nu h^{-2} = 4l^2 \kappa^{-2} h^{2-(1/l)} \quad (5)$$

Then  $l = 1/4$  for constant  $\nu$ . For  $0 < \frac{(x/x_1)}{t_*} \ll 1$

$$I_l \left[ \frac{(x/x_1)}{t_*} \right] \simeq \frac{1}{\Gamma(l+1)} \left[ \frac{(x/x_1)}{2t_*} \right]^l \quad (6)$$

Substituting  $l = 1/4$ ,  $\kappa^{-2}$  and  $I_l$  in Eq.(A.18) we obtain the energy dissipation per unit area

$$D = \frac{1}{2\pi R} g \frac{\partial \Omega}{\partial R} \propto R^{-3} t_*^{-5/4} \exp \left\{ \frac{-[1 + (R/R_1)^2]}{2 t_*} \right\} \quad (7)$$

This contains a sharp rise in the exponential factor, and decays approximately as a power law at late times. The effective temperature of the disk is

$$T = \left( \frac{D}{2\sigma} \right)^{1/4} = c R^{-3/4} t_*^{-5/16} \exp \left\{ \frac{-[1 + (R/R_1)^2]}{8 t_*} \right\} \quad (8)$$

where  $\sigma$  is Stefan-Boltzmann constant and  $c \simeq 3.9 \times 10^7 (\delta m \nu R_1^2)^{1/4}$  (cgs). To find the total luminosity radiated in the disk as a function of time, D must be integrated over the surface of the disk, that is,

$$L(t_*) = \int_{R_0}^{R_1} D 2\pi R dr \quad (2)$$

For the X-ray luminosity  $L_X$  to be determined in the observational energy band from 1 to 20 keV, the temperature in Eq.(8) is substituted in the Planck function

$$F_\epsilon = \frac{2\pi}{h^2 c^2} \frac{\epsilon^3}{e^{\epsilon/kT} - 1} \quad (9)$$

and a numerical integration must be performed over the X-ray band throughout the disk. Since

$$F_\epsilon = F_\epsilon [\epsilon, T(t_*, R)] \quad ,$$

the luminosity is found for each annular section of the disk with thickness  $dR$  at a distance  $R$  from the center and we find the total X-ray luminosity of the disk by integrating.

The observations report the X-ray photon flux in the 1–20 keV band rather than the X-ray luminosity. We use the photon flux

$$N_\epsilon = \frac{2\pi}{h^2 c^2} \frac{\epsilon^2}{e^{\epsilon/kT} - 1} \quad (10)$$

for numerical integration to calculate the total photon flux expected from the disk as a function of time,  $t_*$ . From Eq.(8) the temperature of the inner disk is

$$T_0 = c R_0^{-3/4} t_*^{-5/16} \exp \left\{ \frac{-1}{8 t_*} \right\} \quad (11)$$

since  $R_0/R_1 \ll 1$ . We designate the dimensionless time  $t_*$  corresponding to the maximum of the light curve by  $t_*(\max)$ :

$$\left[ \frac{\partial T_0}{\partial t_*} \right]_{t_*=t_*(\max)} = 0$$

and we find  $t_*(\max) = 0.4$ . If we set  $T_0 = T_0(\max)$  when  $t_* = t_*(\max)$  then

$$c \simeq 1.027 R_0^{3/4} T_0(\max) . \quad (12)$$

Taking the last stable orbit as the inner radius,  $R_0 = 3R_g$  where  $R_g = (2GM/c^2)$ , Eq.(8) becomes

$$T = 1.027 R_0^{3/4} T_0(\max) R^{-3/4} t_*^{-5/16} \times \exp \left\{ \frac{-[1 + (R/R_1)^2]}{8 t_*} \right\} . \quad (13)$$

$T$  is substituted in Eq.(10) and numerical integration is performed over the observed X-ray band (1 – 20 keV) throughout the disk.

The total X-ray photon flux  $n$  received by the detector is

$$n = \frac{\cos i}{2\pi d^2} N \quad (14)$$

where  $N$  is the total X-ray photon flux radiated by the visible surface of the disk,  $d$  is the distance of the source and  $i$  is the inclination angle between the normal of the disk and the line of sight of the observer.

### i. GS 2000+25

The distance of GS 2000+25 is around 2 kpc. The black-hole mass is  $M_X = (5.44 \pm 0.15) \sin^{-3} i M_\odot$  (Harlaftis, Horne & Filippenko 1996). Taking the inclination angle  $47^\circ < i < 75^\circ$ , the mass range is  $6.04 < (M_X/M_\odot) < 13.9$  (Harlaftis, Horne & Filippenko, 1996)

Setting the inner radius at the last stable orbit,  $R_0 = 3R_g$ , the outer radius of the disk  $R_1$  may be chosen  $\sim 10^3 - 10^4$  times the inner radius. Numerical integration for photon flux is not sensitive to the outer radius  $R_1$  as long as  $R_1 \gg R_0$ , since most of the X-ray radiation comes from the inner part of the disk. The maxima of the model light curve and the observed light curve can be matched by adjusting the single parameter  $T_0(\max)$ . This must be done for different masses tracing the possible  $M_X$  range. The values of  $T_0(\max)$  corresponding to different masses and different inner radii are given in Table(2).

Writing the dimensionless time as  $t_* = b t$  we obtain the value of the scale factor  $b$  that gives the best fit (minimum  $\chi^2$ ) between the model and the observed photon count light curves for a grid of mass values in the allowed range. We do this after matching the maxima of the theoretical and the observed light curves, since

there is not enough data during the initial increasing phase of the photon flux. The  $\chi_{min}^2$  values have a decreasing trend with decreasing mass in the mass range of the black-hole. Fig.1 shows the photon flux versus  $t_*$  graph for  $M_X \simeq 13M_\odot$ , with the scale factor  $b$  corresponding to minimum  $\chi^2$ .

For this model

$$t_* = b t = 6 \nu R_1^{-2} t. \quad (15)$$

With  $b \simeq 5.94 \times 10^{-7}$  for  $M_X = 13 M_\odot$ , Eq.(15) gives

$$\nu R_1^{-2} \simeq 8.9 \times 10^{-8} \text{ s}^{-1} . \quad (16)$$

In the  $\alpha$  disk model (Shakura & Sunyaev 1973) the tangential stress can be characterized by the single parameter  $\alpha$  and the kinematic viscosity,  $\nu$ , may be written as

$$\nu = -\alpha \frac{v_s^2}{R \left( \frac{\partial \Omega}{\partial R} \right)} = \frac{2}{3} \alpha \frac{v_s^2}{\Omega} = \frac{2}{3} \alpha \frac{kT}{m_p \Omega} \quad (17)$$

Now the question is when and where the viscosity parameter  $\alpha = (3/2) \nu (m_p \Omega / kT)$  becomes maximum in the disk. Since  $\Omega \propto R^{-3/2}$  and  $kT \propto R^{-3/4}$  we may conclude that  $\alpha$  is always maximum at the inner disk. But  $kT \propto t_*^{-5/16}$  implies that the  $\alpha$  parameter is increasing with time. We follow the luminosity evolution of the disk until the time when the inner disk has cooled down to a temperature characteristic of the quiescent state. The quiescent state temperatures, or temperature upper limits are in the range  $\sim 0.1 - 0.3$  keV for most BSXTs (Tanaka & Shibasaki 1996). We shall use 0.3 keV to derive constraints for  $\alpha$ . The time corresponding to this temperature is already longer than the time of the first mini outburst, after which the fit for the decay following the primary outburst is no longer relevant.

Taking  $kT \sim 0.3$  keV for the quiescent state inner disk temperature and  $\alpha \leq 1$  we obtain the limits

$$\nu \leq 1.8 \times 10^{11} \text{ cm}^2 \text{ s}^{-1}$$

and using Eq.(16)

$$R_1 \leq 1.4 \times 10^9 \text{ cm} \sim 95 R_0.$$

$R_1$  may be less than the outermost radius without effecting the fits as long as the X-ray photon flux coming from  $R > R_1$  is not significant compared to the  $R < R_1$  region.  $R_1$  denotes the location of mass accumulation and release, and is not necessarily identical with the outermost radius. In other words we inject  $\delta m$  at  $R = R_1$  in our idealized model. We obtain  $kT_0(\max) \simeq 0.49$  keV from the fit and  $c \simeq 1.15 \times 10^{12}$  (cgs) from Eq.(12). Using the relation  $c = 4.73 \times 10^7 (\nu R_1^{-2} \delta m)^{1/4}$  (cgs) obtained above for the uniform viscosity model, we have

$$\nu R_1^{-2} \delta m \simeq 3.5 \times 10^{17} \text{ (cgs)} . \quad (18)$$

Substituting the value of  $\nu R_1^{-2}$  from Eq.(16) in Eq.(18) we obtain the amount of mass injected initially at the outer disk

$$\delta m \simeq 3.9 \times 10^{24} \text{ g} . \quad (19)$$

The optically inferred mass transfer rates onto the outer disk of BSXTs are around  $\sim 10^{15} - 10^{16} \text{ g s}^{-1}$  during the quiescent states. These values are similar to those obtained from the long term average,  $\langle \dot{M}_x \rangle$ , of the mass transfer in X-ray outbursts in order of magnitude (Tanaka & Shibazaki 1996, and references therein). This may show that most of the matter accreting onto the disk is accumulated at  $R_1$  during quiescence and is used as a fuel for the next outburst. This is consistent with the observation that  $\dot{M}_x$  during quiescence, which reflects the mass transfer reaching the inner disk, is much less than  $\dot{M}_{\text{opt}}$ . Only one outburst was detected for each of the sources GS 2000+25 and GS/GRS 1124-68, so we use the average accretion rate  $\langle \dot{M}_x \rangle \sim 2 \times 10^{15} \text{ g s}^{-1}$  of another typical BSXT, A0620-00, which has a recurrence time around 58 years (White et al 1984), to estimate the recurrence times of our two sources. From  $t_T \sim \delta m / \langle \dot{M}_x \rangle$  the recurrence time is found to be around 62 years for GS 2000+25.

On the other hand, using  $\alpha = (3/2) \nu (m_p \Omega / kT)$  with  $kT = kT(R_{\text{out}}) \simeq 1.67 \times 10^{-3} \text{ keV}$  where  $R_{\text{out}} \sim 10^3 \times R_0$  it is found that  $\alpha \simeq 5.7 \times 10^{-3}$  for the outer radius. At  $R = R_1$ , where mass accumulation occurs,  $\alpha$  becomes  $3.2 \times 10^{-2}$ . These values correspond to an inner disk temperature of around 0.3 keV. The inner disk temperature decreases to 0.3 keV at  $t \sim 100$  days.

## ii. GS/GRS 1124-68

The distance of GS/GRS 1124-68 is around 3 kpc, the black-hole mass is  $M_X \sim 6M_\odot$  (McClintock et al 1992).  $kT_0(\text{max}) = 0.7 \text{ keV}$  produces the best fit to the Ginga observations of the outburst and decay light curve. For the constant  $\nu$  model, analysis similar to the one described above for GS 2000+25 gives the results

$$\nu R_1^{-2} \simeq 1 \times 10^{-7} \text{ s}^{-1}$$

$$\delta m \simeq 3 \times 10^{24} \text{ g}$$

$$t_{\text{rec}} \simeq 49 \text{ years}$$

$$\nu \leq 8.3 \times 10^{10} \text{ cm}^2 \text{ s}^{-1}$$

$$R_1 \leq 9.1 \times 10^8 \text{ cm} \simeq 172 R_0$$

$$\alpha \leq 5.85(kT)^{-1} R^{-3/2}.$$

For GS/GRS 1124-68 we have taken  $M_X \sim 6M_\odot$  (McClintock et al 1992) and from the best fit we have obtained  $b \sim 6.13 \times 10^{-7}$ . When the inner disk temperature reduces to  $\sim 0.3 \text{ keV}$  the  $\alpha$  values are  $\sim 2 \times 10^{-2}$  and  $\sim 5.3 \times 10^{-3}$  for  $R = R_1$  and  $R = 10^3 R_0$  respectively. The best fitting model for the photon flux history is shown in Fig.2 together with the data. The reduced  $\chi^2$  is found to be 123.7. Although this is a large value, we note that the

magnitudes of the fluctuations of the observed photon flux data about a smooth decay curve are much higher than the errors of the observed data points. As shown in Fig.2 the model reproduces the average rise and decay behavior of the outburst light curve of GS/GRS 1124-68.

## MODEL II: $\nu = \nu(h)$

In this model, we allow  $\nu$  to vary with radius (equivalently, with specific angular momentum,  $h$ ) but not with temperature or time.

### i. GS 2000+25

We adopt the commonly used form of the viscosity parameter prescription  $\alpha = \alpha_0 (z_0/R)^n$ . Cannizzo et al (1995) succeeded to reproduce the exponential type decays of the outbursts of BSXTs employing this form of the viscosity parameter with  $n = 1.5$ . The kinematic viscosity is  $\nu = (2/3)(P/\rho)(\alpha/\Omega)$ . From the hydrostatic equilibrium in the  $z$  direction  $P/\rho \sim z_0^2 \Omega^2$  and  $z_0 \sim v_s/\Omega$ , where  $v_s^2 = kT/m_p$  is the sound speed. Then

$$\nu = \frac{2}{3} \alpha_0 \left( \frac{z_0}{R} \right)^n z_0^2 \Omega .$$

$\nu$  will be independent of temperature only for  $n = -2$ , which gives

$$\nu = \frac{2}{3} \alpha_0 (\Omega R^2) = \frac{2}{3} \alpha_0 h . \quad (20)$$

The specific angular momentum dependence of  $\nu$  is included in the general form of the solution for  $g$  given by Eq.(1). For this choice of  $\nu$  Eq.(5) becomes

$$\frac{1}{2} \frac{(GM)^2}{h} \alpha_0 = 4l^2 \kappa^{-2} h^{2-(1/l)} . \quad (21)$$

Then we obtain

$$l = 1/3$$

$$\kappa^{-2} = \frac{9}{8} \alpha_0 (GM)^2 \quad (22)$$

and

$$t_* = \frac{9}{4} \alpha_0 (GM)^{1/2} \frac{t}{R_1^{3/2}} . \quad (23)$$

Using Eqs.(1), (7), (22) & (23) with  $l = 1/3$  we obtain the energy dissipation rate

$$D \propto t_*^{-4/3} R^{-3} \exp \left[ \frac{-[1 + (R/R_1)^{3/2}]}{2t_*} \right] , \quad (24)$$

and the temperature

$$T = \left( \frac{D}{2\sigma} \right)^{1/4} = c t_*^{-1/3} R^{-3/4} \exp \left[ \frac{-[1 + (R/R_1)^{3/2}]}{8 t_*} \right] . \quad (25)$$

**Table 2.** Results obtained from constant  $\nu$  model for GS 2000+25

$M_X$ ( $M_\odot$ )	$\cos i$	$R_0$ ( $10^6$ cm)	constant $\nu$		$\nu = \nu(h)$	
			$kT_0(\text{max})$ (keV)	$\chi^2_{\text{min}}$	$kT_0(\text{max})$ (keV)	$\chi^2_{\text{min}}$
6	0.26	5.3	0.87	23.5	0.87	19.2
7	0.26	6.2	0.81	21.9	0.80	17.9
8	0.47	7.1	0.66	17.8	0.65	14.6
9	0.53	7.9	0.61	16.3	0.60	13.5
10	0.58	8.8	0.56	15.1	0.57	12.7
11	0.61	9.7	0.53	14.2	0.54	12.0
12	0.64	10.6	0.51	13.4	0.51	11.4
13	0.66	11.5	0.49	12.8	0.49	10.9

where

$$c \simeq 1.1 \times 10^{11} (\delta m \alpha_0 R_1^{-3/2})^{1/4} \text{ (cgs)} . \quad (26)$$

Now we follow the same procedure as we did for the constant  $\nu$  model. The temperature of the inner disk at the time corresponding to the maximum of the outburst is  $T_0(\text{max})$ .  $(\partial T_0 / \partial t_*) = 0$  gives  $t_*(\text{max}) = 0.375$  and  $T(R, t_*)$  becomes

$$T(R, t_*) \simeq T_0(\text{max}) R_0^{3/4} t_*^{-1/3} R^{-3/4} \times \exp \left[ \frac{-[1 + (R/R_1)^{3/2}]}{8 t_*} \right] \quad (27)$$

where  $R_0 = 3R_g = 3(2GM_X/c^2)$ .

**Table 3.** The results obtained from the first model

	GS 2000+25	GS/GRS 1124-68
$R^2 \nu^{-1}$	$\simeq 1 \times 10^7$ sec	$\simeq 1 \times 10^7$ sec
$\delta m$	$\sim 3.9 \times 10^{24}$ g	$\sim 3 \times 10^{24}$ g
trec	$\simeq 62$ years	49 years
$\nu(\text{cm}^2 \text{ s}^{-1})$	$\leq 1.8 \times 10^{11}$	$\leq 8.3 \times 10^{10}$
$R_1$	$\leq 1.4 \times 10^9$ cm	$\leq 9 \times 10^8$ cm
	$\simeq 95R_0$	$\simeq 1.7 \times 10^2 R_0$
$\alpha(R = R_{1\text{max}})$	$\leq 3.2 \times 10^{-2}$	$\leq 2.0 \times 10^{-3}$

Once again we perform the numerical integration to construct the photon flux of the model disk as a function of time. By matching the maxima of the model and the observed light curve, we obtain different  $kT_0(\text{max})$  values for different masses in the range  $6 < M_X/M_\odot < 13.9$ . Later using  $t_* = bT$  we obtain  $b$  values producing minimum  $\chi^2$  for each mass tested. The results are in Table(2). From the best fit we obtain  $M_X = 13M_\odot$ ,  $R_0 = 1.15 \times 10^7$  cm,  $kT_0(\text{max}) = 0.49$  keV, and  $b \simeq 4.63 \times 10^{-7}$ . From Eq.(23)

$$b \simeq 9.34 \times 10^{13} \alpha_0 R_1^{-3/2} \quad (28)$$

we obtain

$$\alpha_0 R_1^{-3/2} = 7.29 \times 10^{-21} \text{ cm}^{-3/2}. \quad (29)$$

The corresponding  $T_0(\text{max})$  produces  $c \simeq 1.17 \times 10^{12}$  and, using Eqs.(26), and (29) we find

$$\begin{aligned} \delta m \alpha_0 R_1^{-3/2} &\simeq 1.6 \times 10^4 \text{ g cm}^{-3/2} \\ \delta m &\simeq 3.3 \times 10^{24} \text{ g}. \end{aligned} \quad (30)$$

Dividing  $\delta m$  by  $\dot{M}_{\text{opt}} \sim \langle \dot{M} \rangle \simeq 2 \times 10^{15} \text{ g s}^{-1}$  we obtain the recurrence time

$$t_r \sim 52 \text{ years}$$

The viscosity parameter  $\alpha$ , with  $n = -2$  and  $z_0 = v_S/\Omega$  is

$$\alpha = \alpha_0 \frac{R^2 \Omega^2}{v_S^2} \quad (31)$$

with  $v_S^2 = kT/m_p$  and  $\Omega = (GM_X)^{1/2} R^{-3/2}$

$$\alpha = \alpha_0 \frac{GM_X m_p}{kT R}. \quad (32)$$

Since  $kT \propto R^{-3/4}$  the viscosity parameter  $\alpha \propto R^{-1/4}$  becomes maximum at the inner disk. Then as we have found in the previous case  $\alpha$  increases with time until  $kT_0 \sim 0.3$  keV. The inner disk temperature reduces to  $kT_0 \sim 0.3$  keV in about 100 days. Eq.(31) with  $\alpha = \alpha_{\text{max}} \simeq 1$ ,  $kT \sim 0.3$  keV and  $R = R_0 = 1.15 \times 10^7$  cm gives  $\alpha_0 \leq 1.9 \times 10^{-6}$ . Using Eq.(29) we find

$$R_1 \leq 5.3 \times 10^9 \text{ cm} \simeq 461 R_0 .$$

As stated before we may consider  $R_1$  to be the radius where the mass accumulates. This  $R_1$  value is nearly 5 times greater than the one obtained in the first model.

When the inner disk temperature is around 0.3 keV using Eq.(27) we find that the temperature is  $\sim 1.7 \times 10^{-3}$  keV at  $R \sim 10^3 R_0$  and  $\sim 3.0 \times 10^{-3}$  keV at  $R = R_1 \sim 461 R_0$ . The corresponding  $\alpha$  values are 0.18 and 0.21 respectively, which are plausible values.

## ii. GS/GRS 1124-68

For this model  $kT_0(\text{max}) = 0.7$  keV produces the best fit to the observed data. Following the steps described

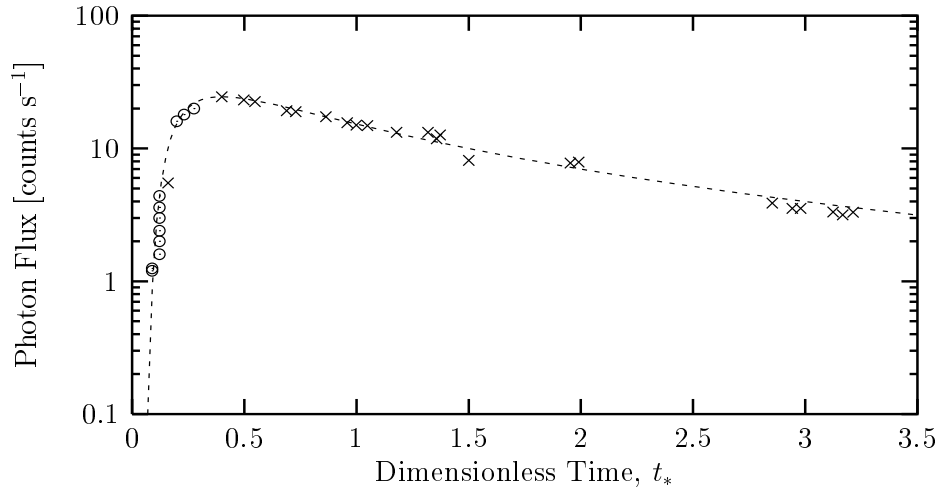


**Fig. 1.** Photon Flux versus dimensionless time for the constant  $\nu$  model (for GS 2000+25). The crosses are Ginga data points obtained from S.Kitamoto. The quoted errors are small compared to the size of the crosses. The circles are extra data points we scaled from Fig.3 in the review paper by Tanaka & Shibazaki (1996). These were not included in fits or the  $\chi^2$  calculations. They are shown here to indicate the success of the model in encompassing the fast rise and turnover phases of the light curve. The dashed line is the LP model fit.

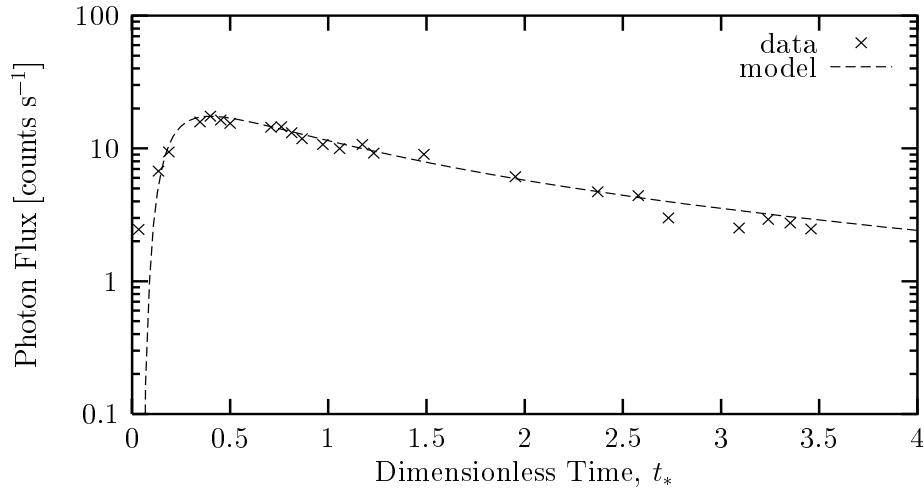


**Fig. 2.** Photon Flux versus dimensionless time for the constant  $\nu$  model (for GS/GRS 1124-68).

above for GS 2000+25 we have obtained a similar fit with the reduced  $\chi^2 = 105.3$  (Fig.4). The results are:

$$\alpha \leq 2.5 \times 10^{-3} (kTR)^{-1}$$

$$\alpha_0 \times R_1^{-3/2} \simeq 8.8 \times 10^{-21} \text{ cm}^{-3/2}$$

$$\delta m \simeq 2.37 \times 10^{24} \text{ g}$$

$$t_{\text{rec}} \simeq 38 \text{ years}$$

$$\alpha_0 \leq 1.9 \times 10^{-6}$$

$$R_1 \leq 3.63 \times 10^9 \text{ cm} \simeq 685 R_0$$

Since  $M_X/R_0 = c^2/6g$  is constant the upper limit for  $\alpha_0$  is the same as that of GS 2000+25 (Eq.32). The recurrence time is similar to that of the first model. When the inner disk temperature reduces to  $\simeq 0.3$  keV the  $\alpha$  values are  $\simeq 0.19$  and  $\simeq 0.17$  for  $R = R_1$  and  $R = 10^3 \times R_0$  respectively.



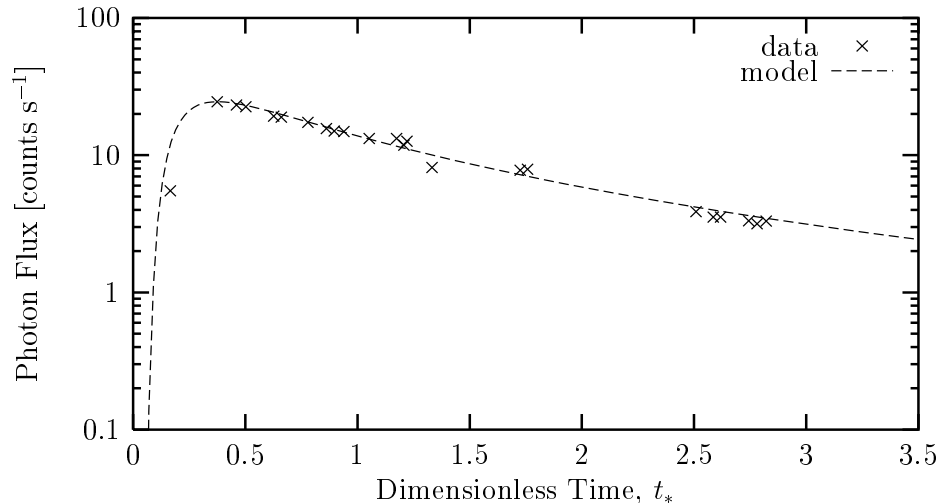


**Fig. 3.** Photon flux versus dimensionless time for the  $\nu = \nu(h)$  model (for GS 2000+25).

From the Roche-lobe geometry the distance from the center of the compact object to the inner Lagrangian point  $L_1$ ,  $R_{L_1} \sim 2 \times 10^{11}$  cm for both sources. When we set  $R_1 \sim R_{L_1}$  we find the  $\alpha_{\max} \ll 1$  which is not plausible. We may conclude that the radius  $R_1$  at which the mass accumulation occurs is around or less than  $2 \times 10^{-2}$  times the disk's outer radius, if the outer radius  $R_{\text{outer}}$  is of the same order as  $R_{L_1}$ . If we take  $R_1 \sim R_{\text{outer}}$ , our inferred values of  $R_1$  would mean that  $R_{L_1}$  is at least fifty times greater than  $R_{\text{outer}}$ .

**Table 4.** The results obtained from the second model

	GS 2000+25	GS/GRS 1124-68
$\delta m$	$\sim 3.3 \times 10^{24}$ g	$\sim 2.4 \times 10^{24}$ g
$t_{\text{rec}}$	$\sim 52$ years	$\sim 38$ years
$\alpha_0$	$\leq 1.9 \times 10^{-6}$	$\leq 1.9 \times 10^{-6}$
$R_1$	$\leq 5.3 \times 10^9$ cm	$\leq 3.6 \times 10^9$ cm
	$\simeq 461 R_0$	$\simeq 685 R_0$
$\alpha(R = R_{1,\text{max}})$	$\leq 0.21$	$\leq 0.19$
$\alpha(R = 10^3 R_0)$	$\leq 0.18$	$\leq 0.17$

### 3. Discussion and Conclusions

We have addressed the general characteristics of the outburst light curves of black-hole soft X-ray transients (BSXTs), through a study of the typical BSXTs GS

2000+25 and GS/GRS 1124-68. The Green's function solution of the accretion disk dynamics model of Lynden-Bell & Pringle (1974) (LP), with a delta function initial mass distribution, produces a rise and decay pattern similar to those of BSXTs. It is most remarkable that this simple dynamical model gives both the rise and the subsequent decay. We have employed this solution adopting a delta function initial mass distribution, a mass  $\delta m$  deposited in a ring at radius  $R_1$  in the disk, for two different time independent viscosity laws. The LP solution restricts the viscosity to be a time independent power law function of the radial distance from the center of the disk.

For the first model we chose a constant kinematic viscosity  $\nu$  for simplicity. For the second model we adopted the commonly used viscosity parameter prescription  $\alpha = \alpha_0 (z_0/R)^n$  and chose  $n = -2$  to remove the time varying temperature dependence of  $\nu$ . This leads to  $\nu = \nu(h)$ , where  $h$  is the specific angular momentum.

For both models  $kT_0(\text{max})$ , the inner disk temperature at the moment that the light curve for photon count rate reaches its maximum, is the free parameter together with  $\cos i$ . We adjusted  $kT_0(\text{max})$  to match the maxima of the model and the observed photon flux light curves. Next, from  $t_* = b t$  where  $t_*$  is dimensionless time and  $t$  is real time, the best fit to the observed photon flux was obtained by adjusting the constant  $b$ . For GS 2000+25 this procedure was performed tracing the possible mass range,  $6M_\odot < M_X < 13.9M_\odot$ , corresponding to the possible inclination angle range,  $47^\circ < i < 75^\circ$  (Harlaftis et al 1996). For GS/GRS 1124-68 the black-hole mass is

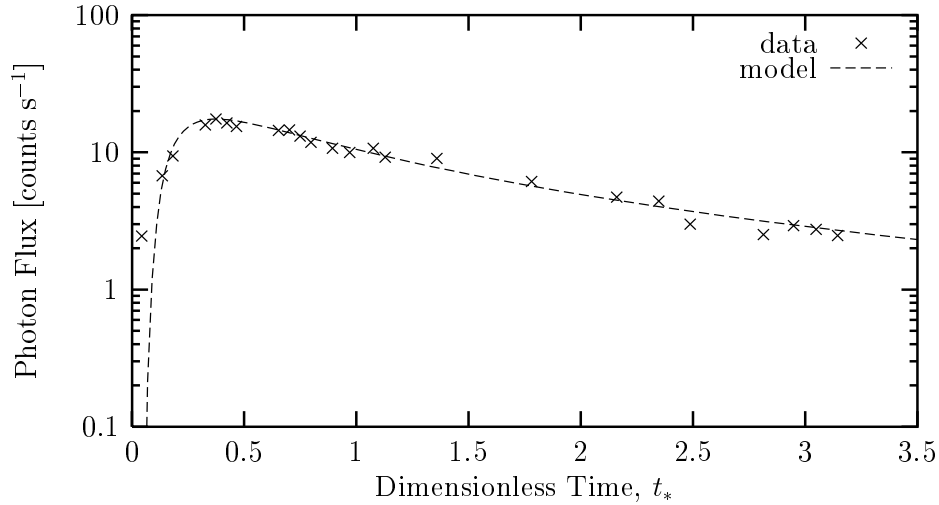


**Fig. 4.** Photon flux versus dimensionless time for the  $\nu = \nu(h)$  model (for GS/GRS 1124-68).

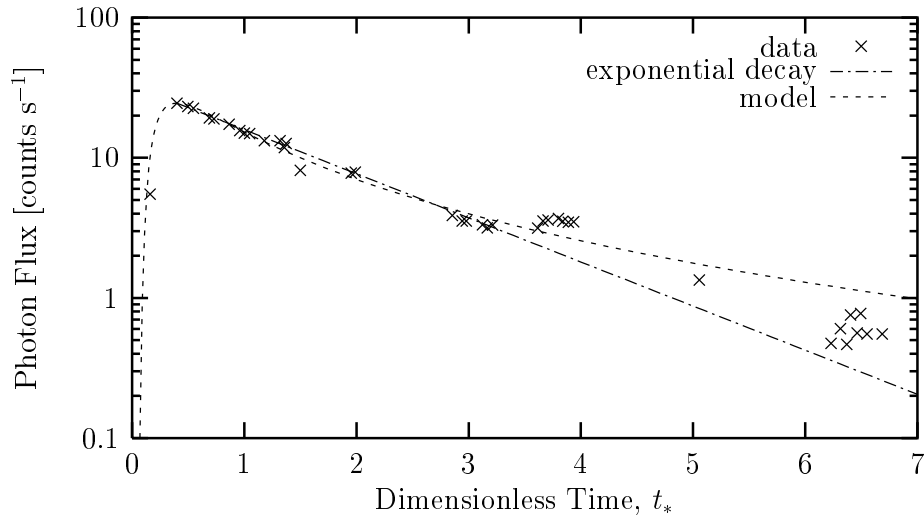


**Fig. 5.** Photon flux versus dimensionless time for the constant  $\nu$  model for GS 2000+25 (dashed line) together with an exponential decay curve (dot-dashed line) with a time constant 30 days. The reduced  $\chi^2_{min}$  values are 5 and 12.8 for the exponential decay and the model respectively, for fits up to the onset of the first mini outburst ( $t_* < 3.5$ ). It is seen that exponential decay models for the mini outburst decays will superpose on the continuing decay of the main outburst. By contrast, LP fits to the mini outbursts require that each mini outburst "zeroes" the continuing decay of the main outburst, and starts with the same initial conditions as the main outburst.

$M_X \sim 6M_\odot$  (McClintock et al 1992). For this source we tried four different  $\cos i$  values (0.25, 0.5, 0.75, 1.0) keeping  $M_X$  constant and followed the same steps to obtain the best fit. The results are in Tables (2–4)

For both sources the fits are applied to the data until the onset of the first mini outburst. The LP model fits the secular decay in the light curve. The large  $\chi^2$  values reflect the excursions about the mean secular decay, which the model does not address. Figs. (1–4) show that both models reproduce the average characteristics of the outburst light curves quite well. The requirement of the model that the kinematic viscosity is independent of time and therefore also of the temperature leads to an  $\alpha$  parameter which increases with decreasing temperature. The usual disk instability models require the opposite trend of  $\alpha$  increasing with increasing temperature. Our time independent viscosity models are artificial and may be considered as an effective representation of real viscosity behavior during the hot states of the accretion disks of BSXTs. Empirically the LP models can explain the rise and the decay following the outburst. Our approach here shows that once sudden mass release is triggered at some  $R_1$ , for example by a disk instability, the subsequent light curve can be understood as the dynamical evolution of the disk with viscosity. It seems plausible that the viscosity mechanism must have a temperature dependence at least to start the outbursts. The success of the model means that the real disk dynamics is insensitive to the temperature dependence of the viscosity, or that a constant effective viscosity LP model is a close approximation to the real luminosity evolution with the integrated effects of variable and temperature dependent viscosity. To investigate the relation between the LP models and disks with variable viscosity is beyond the scope of the present paper, and is to be considered in subsequent work.

The mass dumped in the outburst is  $\delta m \sim 10^{24}$  g in all our model fits, for both sources. This is consistent with accumulation at  $\langle \dot{M}_X \rangle \sim \langle \dot{M}_X \rangle_{0620}$  for recurrence times  $t_r \sim \delta m / \langle \dot{M}_X \rangle \sim 50$  yrs. We expect that the mass release is triggered by a disk instability. The large amounts of mass release  $\delta m$  imply surface densities  $\Sigma \sim (\delta m / R_1^2) \sim 10^4 - 10^5$  g cm $^{-2}$  which are far in excess of the critical (maximum) surface density values for disk instability models,

$$\Sigma_{max} = 11.4 \text{ g cm}^{-2} R_{10}^{1.05} \left( \frac{M}{M_\odot} \right)^{-0.35} \alpha^{-0.86}$$

(Shafer et al 1986). The mass accumulation without triggering an instability then requires small  $\alpha$  values  $\sim 10^{-4} - 10^{-5}$  in the quiescent disk. At such  $\alpha$  the quiescent disk could be optically thin.

There is no complete picture yet which explains all properties of BSXTs, in particular the triggering mechanism for the outbursts which drives the accretion disk from the quiescent state to the outburst and back to

the quiescent state. In a recent study by Cannizzo et al (1995) exponential decay patterns are produced by the disk limit cycle mechanism, but sudden rise of the outbursts and their long recurrence times are not addressed.

The second (and in two sources, third) outbursts have rise and decay patterns which can be fitted with exponentials with time constants similar to those of the main outburst. In addition to this similarity they also pose the problem of understanding the burst repetition time (Augusteijn et al 1993; Chen et al 1993; Mineshige 1994). What is the source of the mass producing the second outburst? The data following the second mini outburst does not allow a detailed fit with the LP model. Assuming that the amplitude of the burst is proportional to the accumulated mass,  $\delta m$ , and scaling with the primary outburst we find  $\delta m$  values are  $\sim 3 \times 10^{23}$  g and  $\sim 2.5 \times 10^{23}$  g for the second mini outbursts in GS/GRS 1124-68 and GS 2000+25 respectively. Using the time interval between the main and the second mini outburst  $\sim 80$  days, we find the extra  $\dot{M}$  to supply the  $\delta m$  of the second mini outburst is  $\sim 4.5 \times 10^{16}$  g s $^{-1}$  for GS/GRS 1124-68 and  $\sim 3.5 \times 10^{16}$  g s $^{-1}$  for GS 2000+25. This is nearly an order of magnitude greater than the long term average accretion rate,  $\langle \dot{M} \rangle$ . Two possibilities may be considered: (1) All the accumulated mass is not released during the main outburst. The mass released in the second outburst is "leftover mass" and not accumulated between the main outburst and the second outburst. (2) The mass flow from the companion is enhanced by the X-rays coming from the inner disk in the outburst; or both possibilities run together. The X-ray heating of the disk may be important to trigger the mini outbursts whatever the source of the mass creating the second and the third instabilities.

The time between the main and mini outbursts ( $\sim$  few months) must be a characteristic time scale of the "trigger". The response time scale of the upper atmosphere of the secondary is too short ( $\lesssim 10^3$  s) (Chen et al 1993 (CLG)) while the viscous time scale is of the order of a week. The shielding of the region around the inner Lagrangian point,  $L_1$ , has been proposed to explain this time interval (CLG). If the geometrical shielding should end gradually, the abrupt rise of the first mini outburst at a particular time remains unexplained. Two different approaches were proposed by Mineshige (1994). An optically thick Compton cloud above and below the disk which becomes optically thin in a very short time scale just before the first mini outburst may explain the first mini outburst by the response of the companion to the X-rays coming from the inner disk. Alternatively a second thermal instability would be triggered at the outer disk when the strong X-ray heating of the disk has raised the temperature and decreased the critical density for the trigger sufficiently (transient recession of the cooling front). In the former scenario one still has to explain the secondary mini outburst by invoking a different mechanism, and also exhibits similar rise and decay time scales. Similar time interval and

characteristics of all the outbursts seem to imply a unique mechanism responsible for the triggering of the outbursts.

It is well known that simple exponential decays after the outburst maximum describe the data well. The mini outburst decays can also be fitted with exponential decays with the same time constants as required by the main outburst (Fig.5). However, the fast rise and the exponential decays (FRED) are put together as separate pieces of the fit rather than being part of a single dynamical model as in the present model. Our LP models fit the main outburst decay quite well. There is an interesting difference from FRED models when it comes to trying to fit the data incorporating the mini outbursts and their decays. In FRED models, the data stream can be fitted well by a superposition of FRED models for the main outburst and the mini outbursts. For our LP model fits, by contrast, when the fit to the main outburst data is extended past the mini outburst(s), it is seen that the model gives a count rate that is greater than the observed count rates, the deviation starting from the onset of the mini outburst. If it is assumed that the ongoing relaxation in the disk after the main outburst is stopped, and the onset of the mini outburst involves an instability that resets the disk to conditions similar to sudden mass release from a local accumulation, then the LP model can be applied to the mini outburst(s) and their decays.

Augusteijn et al (1993) drew attention to the similarity of the main outburst decay, and the mini outburst decays. They related this to a feed-back model invoking modulation of the mass transfer from the companion by irradiation from the outburst. The present approach identifies the similarity with repeated conditions of mass accumulation and release in the disk itself. The trigger of the mass release could be a disk instability. The similarity of main outburst and mini outbursts, requires small scale repetitions of the main outburst with similar initial conditions, rather than superposition or convolution with the disk state as evolved from the main outburst's decay. The presently available data do not allow a detailed fit of the mini outbursts with the LP models.

The behavior of GS 2000+25 and GS/GRS 1124-68 are similar to those of A0620-00, and GRO J0422+32. The conclusions may be extended to them as well. These ideas will be developed and a similar detailed study for the other sources will also be attempted in future work.

**Acknowledgements** This work started from discussions with our late colleague Jacob Shaham. We thank S.Kitamoto for providing GINGA outburst data for the sources GS 2000+25 and GS/GRS 1124-68, and the referee S.Mineshige for his helpful comments. We thank the Scientific and Technical Research Council of Turkey, TÜBİTAK, for support through the grant TBAG Ü-18. Ü.Ertan thanks TÜBİTAK for a doctoral scholarship. M.A.Alpar acknowledges support from the Turkish Academy of Sciences.

## References

- Augusteijn T., Kuulkers E., Shaham J., 1993, A&A 279, L13  
 Bath G.T., Pringle J.E., 1981, MNRAS 194, 967  
 Cannizzo J.K., *Accretion Disks in Compact Stellar Systems*, 1992 Ed. J.C.Wheeler 6-40  
 Cannizzo J.K., 1994, ApJ 435, 389  
 Cannizzo J.K., Chen W., Livio M., 1995, ApJ 454, 880  
 Chen W., Livio M., Gehrels N., 1993, ApJ 408, L5  
 Hameury J.M., King A.R., Lasota J.P., 1986, A&A 162, 71  
 Hameury J.M., King A.R., Lasota J.P., 1987, A&A 171, 140  
 Hameury J.M., King A.R., Lasota J.P., 1988, A&A 192, 187  
 Hameury J.M., King A.R., Lasota J.P., 1990, A&A 353, 585  
 Harlaftis E.T., Horne K., September 1996, PASP  
 Lasota J.P., 1996, *Compact Stars in Binaries*, IAU Symp. eds. J. van Paradijs, E.P.J. van den Heuvel p.43  
 Lasota J.P., Narayan R., Yi I., 1996, A&A 314, 813  
 Lynden-Bell D., Pringle J.E., 1974, MNRAS 168, 603 (LP)  
 McClintock J.E., Bailyn C.D., Remillard R.A., 1992, IAU Circ. No. 5499  
 McClintock J.E., Horne K., Remillard R.A., 1995, ApJ 422, 358  
 Meyer F., Meyer-Hofmeister E., 1981, A&A 104, L10  
 Meyer F., Meyer-Hofmeister E., 1983, A&A 128, 42  
 Mineshige S., 1994, ApJ 431, L99  
 Mineshige S., Wheeler J.C., 1989, ApJ 343, 241  
 Narayan R., McClintock J.E., Yi I., 1996, ApJ 457, 821  
 Shafter A.W., Wheeler J.C., Cannizzo J.K., 1986, ApJ 305, 261  
 Shakura N.I., Sunyaev R.A., 1973, A&A 24, 337  
 Tanaka Y, X-Ray Binaries and Recycled Pulsars, eds. E.P.J. van den Heuvel and S.A. Rappaport, 1992, p.37  
 Tanaka Y., Shibazaki N., 1996, ARA&A Vol.34  
 Tsunemi H., Kitamoto S., Okamura S., Roussel-Dupré D., 1989, ApJ 337, L81  
 van Paradijs J., 1995, X-Ray Binaries, eds. W.H.G. Lewin, J. van Paradijs, E.P.J. van den Heuvel p.536  
 White N.E., Kaluzienski L.J., Swank J.L. 1984 High-Energy Transients in Astrophysics, Eds. S.Woosley, p.31

## Appendix

Here we summarize, following Lynden-Bell & Pringle 1974 (LP), the general arguments of the angular momentum and the energy flow in the thin accretion disks. Consider a thin annular section of a disk of width  $dR$  at radius  $R$  from the center. The torque or couple acting on the inner edge of the annulus is

$$g(R) = 2\pi R^2 \nu \Sigma 2 A(R). \quad (A.1)$$

where  $A(R)$  is the local rate of shearing

$$A = -\frac{1}{2} R \frac{d\Omega}{dR}. \quad (A.2)$$

$\Omega$  is the angular velocity about the center,  $\nu(R)$  is the kinematic viscosity and  $\Sigma(R)$  is the surface density. Viscous forces are proportional to velocity gradients, and viscous torques are proportional to angular velocity gradients (shear).

We may write the equation of motion of the annulus at radius  $R$  in the form

$$\frac{D}{Dt} (h dm) = -\frac{\partial g}{\partial R} dR. \quad (A.3)$$

where  $h = \Omega R^2$ ,  $dm = \Sigma 2\pi R dR$  and  $(D/Dt) = (\partial/\partial t) + \mathbf{U} \cdot \nabla$  is the total (convective or Lagrangian) time derivative following a fluid element. Eq.(A.3) states that rate of change of angular momentum is given by the torque.

Since  $D(dm)/Dt = 0$

$$2\pi R \Sigma \frac{Dh}{Dt} = -\frac{\partial g}{\partial R} = \frac{\partial}{\partial R} \left( 2\pi R^3 \Sigma \nu \frac{\partial \Omega}{\partial R} \right). \quad (A.4)$$

If the specific angular momentum  $h = \Omega R^2$  is independent of time Eq.(A.4) becomes

$$F \frac{dh}{dR} = -\frac{\partial g}{\partial R} = \frac{\partial}{\partial R} \left( 4\pi R^3 \Sigma \nu \frac{\partial \Omega}{\partial R} \right) \quad (A.5)$$

where  $F$  is the outward flux of matter through the radius  $R$ . For a Keplerian disk we can take

$$\Omega = (GM)^{1/2} R^{-3/2} \quad (A.6)$$

where  $M$  is the mass of the star at the center of the disk.

Energy generated by the matter flowing into the gravitational well is redistributed or convected by  $g\Omega$ , and the remainder is dissipated by

$$D = \frac{1}{2\pi R} g \left( -\frac{d\Omega}{dR} \right). \quad (A.7)$$

The continuity equation for the fluid is

$$\frac{\partial \Sigma}{\partial t} + \frac{1}{2\pi R} \frac{\partial F}{\partial R} = 0 \quad (A.8)$$

where  $\Sigma$  is the surface density of the disk. Using Eqs.(A.4&A.8)

$$\frac{\partial^2 g}{\partial h^2} = \frac{\partial}{\partial t} \left[ \frac{g}{2A\nu R (dh/dR)} \right] \quad (A.9)$$

is obtained. Lynden-Bell & Pringle (1974) express the denominator as

$$2A\nu R \frac{dh}{dR} = 4l^2 \kappa^{-2} h^{2-(1/l)} \quad (A.10)$$

where  $\kappa$  and  $l$  are constants. Eq.(A.10) is valid as long as  $\nu$  is constant or varies as a function of  $R$ , and can be used to parametrize the  $\nu$  and  $h$  laws. Eq.(A.9) reduces to

$$\frac{\partial^2 g}{\partial h^2} = \frac{1}{4} \left( \frac{\kappa}{l} \right)^2 h^{(1/l)-2} \frac{\partial g}{\partial t}. \quad (A.11)$$

Resolving Eq.(A.11) into modes where  $g \propto e^{-st}$  and setting  $k^2 = \kappa^2 s$

$$\frac{\partial^2 g}{\partial h^2} + \frac{1}{4} \left( \frac{k^2}{l^2} \right) h^{(1/l)-2} g = 0 \quad (A.12)$$

and changing the variables  $x = h^{1/2l}$  and  $g_1 = x^{-l} g$  in Eq.(A.12) gives a transformation of Bessel's equation

$$\frac{\partial^2 g_1}{\partial x^2} + x^{-1} \frac{\partial g_1}{\partial x} + \left( k^2 - \frac{l^2}{x^2} \right) g_1 = 0$$

with solution given by

$$g = e^{-st} (kx)^l [A(k)J_l(kx) + B(k)J_{-l}(kx)]. \quad (A.13)$$

The general solution of Eq.(A.11) is given by a convolution of such modes. Then

$$g = \int_0^\infty \exp\left(-\frac{k^2 t}{\kappa^2}\right) (kx)^l [A(k)J_l + B(k)J_{-l}] dk \quad (A.14)$$

where  $B(k)=0$  for the central couple to be zero,  $g(x=0)=0$ .  $A(k)$  is given by the inverse transform

$$A(k) = \int_0^\infty g(h,0) J_l(kx) (kx)^{1-l} dx. \quad (A.15)$$

When there is no central couple as in the case of BSXTs any solution may be considered as made up of elementary solutions whose initial density distributions are of the form

$$\Sigma(R_1, R, 0) = (2\pi R_1)^{-1} \delta(R - R_1) \quad (A.16)$$

and the corresponding couple is

$$g(h_1, h, 0) = 2l \kappa^{-2} x_1^{2l-1} \delta(x - x_1). \quad (A.17)$$

For the special initial condition in Eq.(A.17), using Eq.(A.15)

$$A(k) = 2l \kappa^{-2} x_1^l k^{1-l} J_l(kx_1).$$

Substituting  $A(k)$  in Eq.(A.14) with  $B(k)=0$

$$g = 2l \kappa^{-2} \frac{(x_1 x)^l}{x_1^2 t_*} \exp - \left[ \frac{(x_1 - x)^2}{2t_* x_1^2} \right] F_l \left( \frac{x/x_1}{t_*} \right) \quad (A.18)$$

where  $t_* = 2\kappa^{-2}t/x_1^2$ ,  $F_l(z) = e^{-z} I_l(z)$  and  $I_l(z)$  is the Bessel function of imaginary argument.

For the general initial conditions  $g(h_1, 0)$  the general solution is given by

$$g(h, t) = \int_0^\infty g(x_1^{2l}, 0) \kappa^{-2} \frac{x_1^{-(1+l)} x^l}{t_*} \exp - \left[ \frac{(x_1 - x)^2}{2t_* x_1^2} \right] \\ \times F_l \left( \frac{x/x_1}{t_*} \right) dx_1 \quad (A.19)$$

(Lynden-Bell & Pringle, 1974)(LP). Substituting this solution in Eq.(A.7) and integrating throughout the disk one can obtain the total luminosity of the disk for the general initial conditions  $g(h_1, 0)$ . Instead we use the solution given by Eq.(A.18) which represents a delta function initial mass distribution at a radial distance  $R = R_1$ , which may be considered as the outer radius of the disk. The luminosity curve obtained by LP with a delta function initial mass distribution is very similar to those of BSXTs.